ТUП

Investigation of multispectral imaging algorithm for temperature determination on a numerical experiment platform in Laser-based Powder Bed fusion of Metals

Untersuchung des multispektralen Bildgebungsverfahrens zur Temperaturbestimmung auf einer numerischen Experimentierplattform beim Laser-basierten Pulverbett-Schmelzverfahren von Metallen.

Semester Thesis

at the Department of Mechanical Engineering of the Technical University of Munich

Supervised by	Prof. Dr.-Ing. Katrin Wudy
	M.Sc. Ruihang Dai
	Laser-based Additive Manufacturing
Submitted by	Zhaoyong Wang
	Connollystr.3
	80809 München
Submitted on	July 31, 2023 in Garching

Scope of Work

Title of the Semester Thesis:

Investigation of multispectral imaging algorithm for temperature determination on a numerical experiment platform in Laser-based Powder Bed fusion of Metals

Author:	B.Sc. Zhaoyong Wang	**Supervisor:**	M.Sc. Ruihang Dai
Issuance:	15.03.2023	**Submission:**	31.12.2021

Setting:

Laser-based Powder Bed Fusion of Metals (PBF-LB/M) is an additive manufacturing process which produces components with a laser by successively melting metal powders applied in layers. This additive manufacturing process offers the advantage of a complex lightweight design. However, complicated thermal histories during laser-metal interaction can lead to process defects such as keyholing. Since the process is thermally driven, acquiring the absolute temperature distribution in the laser-material interaction zone is vital to gain a deeper understanding of the process. However, no measurement system in PBF-LB/M is currently available to determine the absolute temperature due to unknown emissivity. Multispectral Imaging (MSI) has the potential to determine the absolute temperature and emissivity simultaneously by capturing multiple wavelengths of radiance from the melt pool.

Objective:

This work aims to optimize the MSI algorithm to determine the absolute temperature accurately. Since the mapping between the digital value and radiance still needs to be investigated, direct optimization of the MSI algorithm based on the experimental data is challenging. Therefore, the first step is to develop a virtual experiment to obtain "ideal" radiance determined by the given temperature distribution and emissivity. This way, the MSI algorithm can be optimized based on the input and calculated temperature and emissivity. The virtual experiment platform will also allow for the investigation of various temperature distributions and emissivity models in a time- and cost-efficient manner.

Methodology:

The content of the present thesis can be subdivided into the following tasks

- Literature review regarding MSI, material emissivity model and curve fitting algorithms

- Development of a virtual experiment platform

- Generate virtual experiments with various emissivity models and temperature fields

- Optimization of the MSI algorithm based on virtual experiments

- Scientific documentation of the results

Declaration

I hereby confirm that this semester thesis was written independently by myself without the use of any sources beyond those cited, and all passages and ideas taken from other sources are cited accordingly.

....
Location, Date

....
Signature

With the supervision of Mr. Zhaoyong Wang by Mr. Ruihang Dai intellectual property of the Professorship Laser-based Additive Manufacturing (LBAM) flows into this work. A publication of the work or a passing on to third parties requires the permission of the head of the professorship. I agree to the archiving of the printed thesis in the LBAM library (which is only accessible to LBAM staff) and in LBAM's digital thesis database as a PDF document.

....
Location, Date

....
Signature

Abstract

temperature is one of the most important parameters in PBF-LB/M. so, monitoring the temperature at melt pool necessary. in oder to archieve this, a numerical experiment platform is formed. then parameter is calculated

Zusammenfassung

Hier könnte Ihre Kurzzusammenfassung stehen.

Contents

1 LaTeX-Tutorial

Dieses Tutorial liefert eine Kurzeinführung in die Verwendung von Latex.

1.1 Titelseite

Die Titelseite wird in ./main.tex definiert. Der Studienarbeitstyp wird durch Ein- und Auskommentieren der Befehle

- `\IWBstudentthesisTitlePageCustomMastersThesis`,
- `\IWBstudentthesisTitlePageCustomBachelorsThesis` und
- `\IWBstudentthesisTitlePageCustomSemesterThesis`

ausgewählt und die Seite entsprechend der Argumente gesetzt. Die Professoren und Lehrstuhle können mittels der Makros

- `\IWBnamesProfReinhart \newline \IWBlangChairMWIWBLBM` oder
- `\IWBnamesProfZaeh \newline \IWBlangChairMWIWBLWF`

ausgewählt werden.

1.2 Zitation

Zum Zitieren stehen die Standartbefehle `\textcite` und `\parencite` zur Verfügung. Soll der Autorename im Satz verwendet werden, eignet sich ersteres, z.B. **Bayerlein2018** bezieht sich auf **Bayerlein2016469**. Soll das Zitat in Klammern nach die Aussage gestellt werden empfiehlt sich zweiteres [**Zaeh2018385**]. Sammelzitationen am Satzende schreiben sich wie folgt [**Kleinwort2018658**, **Kleinwort20189**, **Kleinwort2018631**]. Die Zitation von Online-Quellen kann schwierig sein, da nicht immer der Autor und das Erscheinungsjahr verfügbar sind. Vergleicht man **Heuss2018** und **iwb-Startseite**, stellt man fest, dass bei zweiteren der Seitentitel statt des bekannten Schemas eingesetzt wird.

Normen werden als dargestellt. Im Bibtex-Export des verwendeten Literaturverwaltungsprogramm sind bestimmte Einstellungen vorzunehmen. Dokumententyp ist "@book" mit folgenden Einträgen:

- Normtyp und Nummer als "title"
- Langtitel als "subtitle"
- Verlag als "publisher"
- Jahr als "date"
- "author" darf nicht belegt werden!

1.3 Abkürzungen

In ./source/abbreviations.tex können Abkürzungen definiert werden. Es gibt Besonderheiten zu Ausdrücken, deren Pluralendung nicht auf s endet. Hier müssen ggf. Kurz- und Langformen des Ausdrucks auch für den Plural definiert werden.

- `\gls{ros}`: schreibt beim ersten Auftreten im Dokument ausführlich Robot Operating System (ROS), ab dem zweiten Auftreten wird abgekürzt ROS
- `\glspl{ap}` verwendet den Plural in Langform Arbeitspakete (APs) und danach in Kurzform APs

1.4 Glossar

In ./source/glossary.tex können Begriffe erklärt, abgegrenzt oder definiert werden. Begriffe erhalten einen Namen und eine Beschreibung als Glossareintrag sowie ein Lable zum Referenzieren im Text. Ein Glossar ist Optional.

- `\gls{latex}`: Schreibt den Namen aus dem Glossarverzeichnis mit Verweis auf den Glossareintrag Latex

1.5 Abbildungen

Graphiken und Bilder können in beliebigen Dateiformaten eingebunden werden, vergleiche fig. 1. Vektorgraphiken sind im Allgemeinen Pixelgraphiken in Schärfe und Speicherbedarf überlegen.

Figure 1: Beschreibung des Bilds. Außerdem machen wir nun die Bildunterschrift unnötig lang um die Formatierung zu testen.
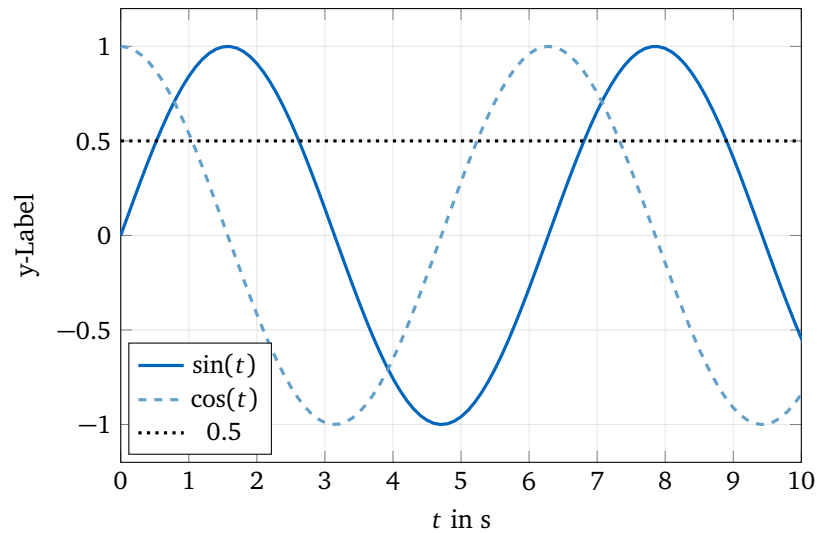
Figure 2: Beschreibung des Plots. Außerdem machen wir nun die Bildunterschrift unnötig lang um die Formatierung zu testen.

Für Nutzer mit perfektionistischen Anspruch empfiehlt sich die Nutzung von Ti*k*Z. Vorteil ist, dass die Erzeugung von Daten und die Darstellung komplett getrennt werden. Die Darstellung erfolgt einheitlich gemäß eines generischen Mark-Ups, vergleiche figs. 2 and 3.

Figure 3: Beschreibung des Plots. Außerdem machen wir nun die Bildunterschrift unnötig lang um die Formatierung zu testen.

2 Introduction

Additive Manufacturing (AM) is a different type of processing technology to conventional manufacturing methods. Instead of removing material from the raw part, additive manufactoring is usually described as "a process of joining materials to make objects layer by layer or element by element"[1]. It is a useful method for reducing the the duration from product design to product manufacturing and imporving the material utilization[2].

There are several AM technologies that can be sorted into different categories. Laser-based Powder Bed Fusion of Metals (PBF-LB/M), which also called Selective Laser Sintering (SLS), is one of the powder based AM processes[3]. In this process, a laser beam with high energy density is focused onto the surface of a metal powder bed, which was heated up to a temperature near the melt temperature. Then, the metal powder is melted and form the upper surface of the object. Last, the building platform will go downwards to build next layer. This process will be repeated until the desired object is built[4].

Since the process is based on the phase change of materials, processing parameters such as laser power, layer thickness, hatch distance and scanning strategies are critical for producing dense materials, minimize defects, improve surface quality and build rate[5]. The common denominator between them is that the parameters of the process are varied by controlling the temperature profile of the metal powder[2]. Thus, the importance of obtaining the temperature information on the surface layer is high.

The solidification front of metal powders moves with a high velocity (generally $0.01 \sim 10\,\mathrm{m/s}$)[6], the cooling rate of material is normally at range of $10^5 \sim 10^6\,\mathrm{K/m}$[5]. Thus, a contactless temperature measurement is required to obtain the temperature of the surface area.

Two different methods is used for monitoring the surface temperature in recent studies, namely conventional infrared irradiation temperature measurement methods and multi-wavelength techniques[7]. Infrared irradiation technique is cost-effective, but it requires information about the emissivity of the material[8]. On the contrary, a multi-color pyrometer with a specific wavelength range could be used in the case of changing emissivity[9]. In this thesis, a virtual experiment platform using a multispectral imaging algorithm is developed to simulate the output behavior of a spectral pyrometer.

After obtaining the radiation image, a curve fit algorithm is applied to estimate the temperature field of the image and emissivity field simultaneously. This semester thesis aims to develope a stable temperature estimation program based on curve-fit algorithm. With the results obtained from the virtual experiment platform, the performance of the temperature estimation algorithm is verified.

3 State of the art

haha[10]

3.1 Process monitoring

3.2 Multispectral imaging

3.3 Emissivity model

3.4 Temperature field in Laser-based Powder Bed Fusion

3.5 Motivation of this thesis

4 Theory and methodology

As mentioned in previous sections, forming a virtual experiment platform is necessary for investigating the temperature estimation algorithm. So, a virtual experiment platform is developed based on Planks'law, then, a virtual multi-spectral pyrometer is applied to obtain the digital value (also called image).

4.1 Physical value of radiation

Radiation is emitted from any object with a temperature above $0\,\text{K}$. In equation 4.1 can be found, that the radiation depends on the black body radiation $B(\lambda, T)$ and emissivity $\varepsilon(\lambda, T)$. Both value are temperature T and wavelength λ dependent.

$$L(\lambda, T) = B(\lambda, T) \cdot \varepsilon(\lambda, T) \tag{4.1}$$

By Plank's Law, black body radiation can be described in equation 4.2, with absolute temperature T, wavelength λ, speed of light c, Plank constant h and Boltzmann constant k_B. Black body radiation is irrelevant to the material itself, all materials at the same temperature have the same spectral black body radiation.

$$B(\lambda, T) = \frac{2hc^2}{\lambda^5} \cdot \left[\exp\left(\frac{hc}{\lambda k_B T} \right) - 1 \right]^{-1} \tag{4.2}$$

On the contrary, emissivity varies from material to material. It is the ratio of the actual spectral intensity emitted by the object to the spectral intensity of the black body radiation. In the study of radiation, two idealized material models are generally used to describe the idealized properties of radiation, namely black body and grey body.

Black-body material emits electromagnetic black body radiation, which is irrelevant to the wavelength of the radiation and the shape of the material[11]. Which also means the emissivity of a black body is constantly 1. It could be used to validate the temperature estimation algorithm in following sections.

Unlike black-body materials, grey-body materials have an emissivity between 0 and 1. Not all of the thermal radiation could be emitted to the outside of the material. Different from normal materials, the emissivity of a grey-body material is irrelevant to the wavelength of radiation.

In Fig.4 can be found, that the real spectral intensity of a normal material is lower than the black body spectral intensity. And the emissivity of the material varies with the increase of the radiation wavelength.

It can be seen that the construction of a reliable emissivity model is crucial to the accuracy of the virtual experimental platform. It is the key component used to generate the experimental data.
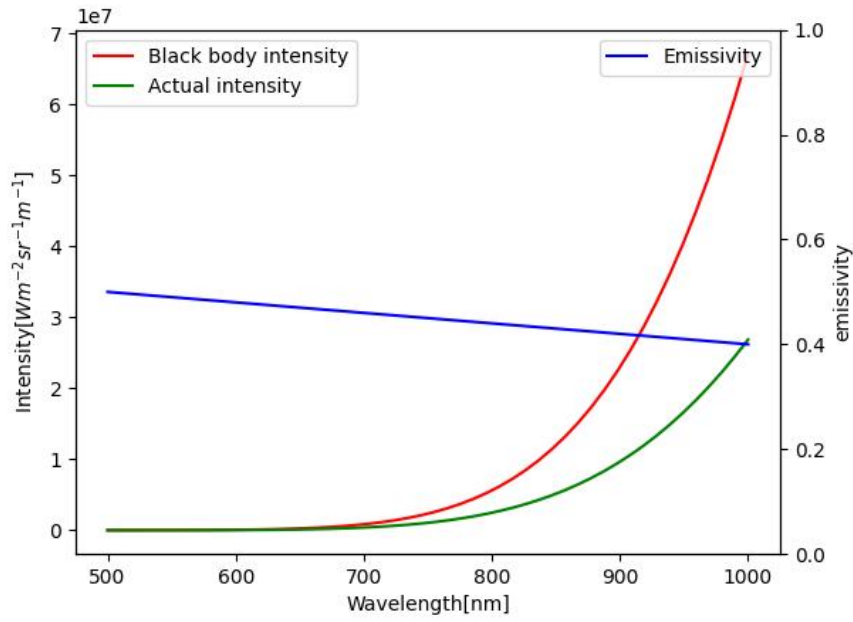
Figure 4: Black body radiation, emissivity and real radiation of an example normal material at $1000K$

4.2 Virtual experiment platform

After obtaining the physical spectral intensity of the material, a virtual experiment platform is used to transform the physical value into digital value, which simulate the behavior of a real spectral pyrometer. As described in Fig.5a, a camera with a lens system focused on the surface of the powder bed is resonsible for obtaining spectral radiation of the heated metal powder. It can be seen from Fig.5b, each pixel of the sensor contains 8 filters and thus be able to obtain 8 intensity digital values in different channels. Thus, a virtual experiment platform with the same structure as the real experiment platform is built.
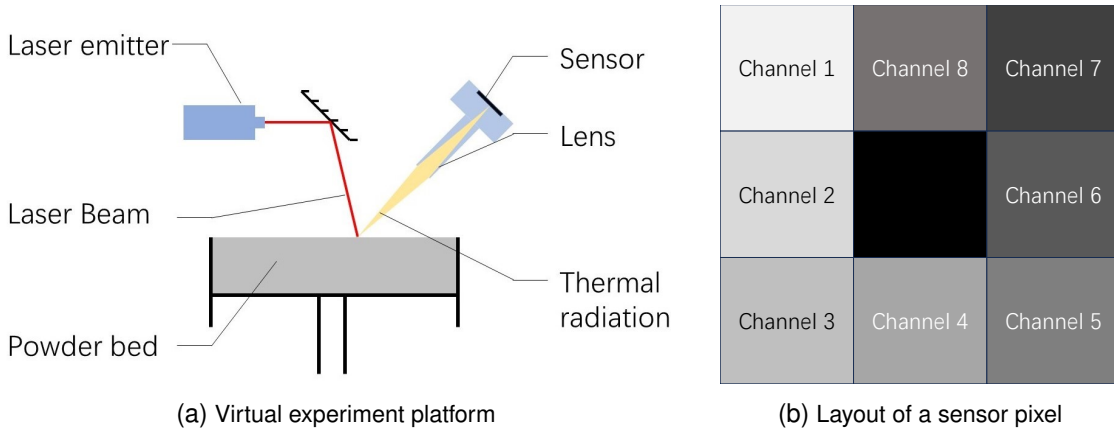

(a) Virtual experiment platform

(b) Layout of a sensor pixel

Figure 5: Structure of the virtual experiment platform and Layout of a sensor pixel

4.3   Camera model

It can be found in Fig.5, The thermal radiation is emitted from the surface of powder bed, and passes through the lens system of the camera, finally, it reaches the sensor and be converted into digital values. The simplified process can be seen in Fig.6. As dA_m is the area of the focused surface and dA_{pixel} the area of the pixel in camera system, n_m is the normal vector of the surface.
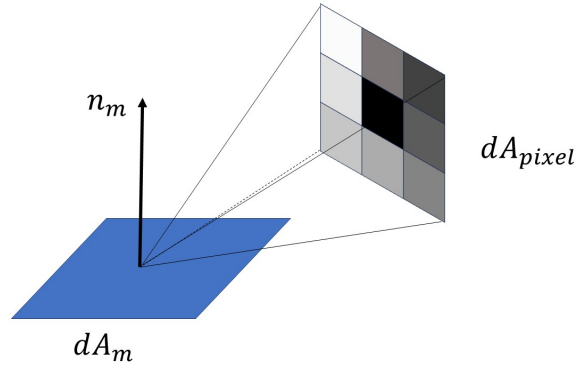

Figure 6: Radiative exchange between camera system and powder bed

4.3.1   Frequency response

After obtaining the virtual experiment platform and knowing the external setup of the sensor, the internal effects of the camera system should also be taken into account in the complete virtual experiment platform.

In order to simulate real camera system, the frequency response of sensor and lens should be considered. In real camera systems, all spectral radiation will pass through the lens system of camera. Since the lens system is not an idealized system, the effect of the lens system is not negligible.
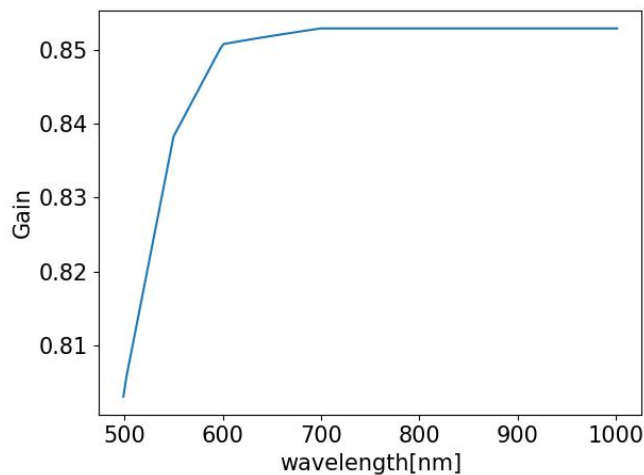

Figure 7: Frequency response of the lens system

It can be found in Fig.7 that system gain of lens system is not constant. In the wavelength range of 500 to 700 nanometers, the lens is more sensitive to the radiation with long

wavelength. With the increasing wavelength, the system gain of the lens system keep constant at 0.853.

In addition to the fact that the lens system respond differently to radiation with different wavelengths, the sensor of the camera also have wavelength-dependent quantum efficiency. As mentioned in previous section, the acquisition of the spectral intensity by the sensor for different channels is based on the filter before the pixels.

Fig.8 shows the quantum efficiency of the camera sensor in different channels. Unlike an ideal sensor that receives only single wavelength radiation, the intensity information received by a real sensor is a combination of a spectral radiation and 8 filters with different frequency responses. Thus, the camera system is able to obtain the spectral radiation intensity in 8 channels simutaneously.
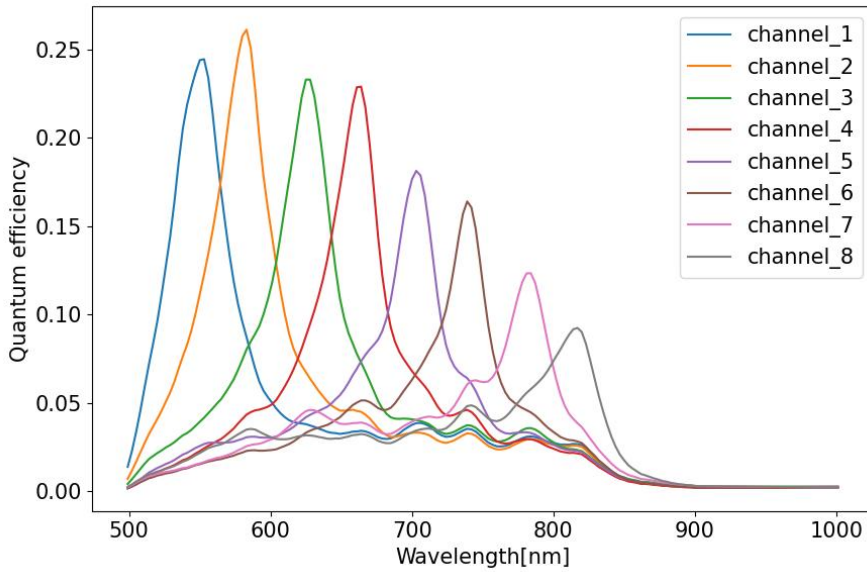

Figure 8: Quantum efficiency of camera system in each channel

To make the virtual experiment platform more comparable to real experiments, it can be concluded that it is necessary to build a camera model that incorporates the effects of sensor quantum efficiency and lens transparency. Then, the physical value of the spectral radiation intensity could be calculated accurately by the digital value of spectral radiation intensity obtained from the virtual experiment platform.

4.3.2 Integration method

As a result, the process of converting the physical values of radiation intensity into digital values needs to be accurately reproduced. Since the total efficiency of the camera (η_{camera}) was delivered by quantum efficiency ($\eta_{quantum}$) of the sensor and transparency of the lens system (τ_{lens}), the mathematical relationship could be described in Eq.4.3.

$$\eta_{camera} = \eta_{quantum} \cdot \tau_{lens} \tag{4.3}$$

Fig.9 shows the relationship between the incoming spectral radiation intensity and actual captured spectral radiation intensity by the camera system. It can be found that the wavelength of the spectral radiation intensity actually received by the sensor deviates from the wavelength of the spectral radiation intensity it supposed to receive.
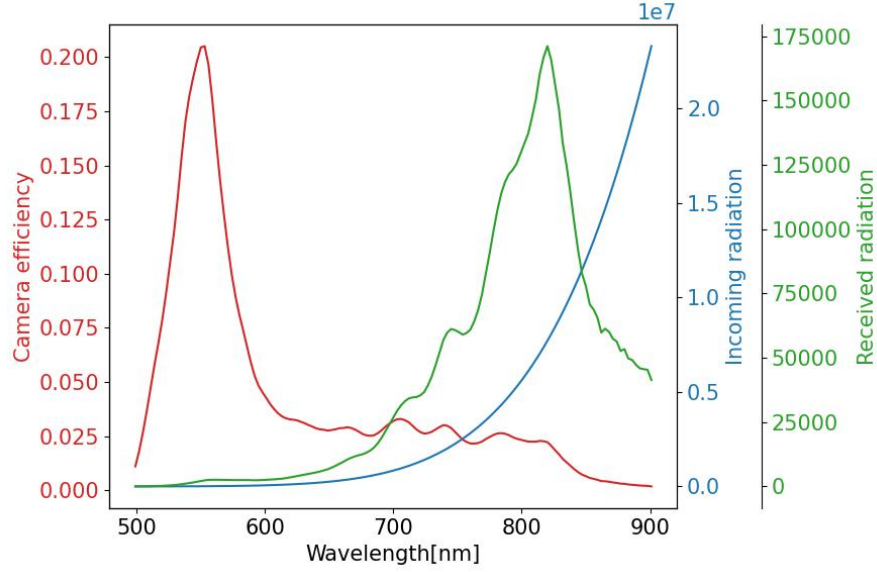
Figure 9: Actual received spectral radiation intensity by channel 1 at 1000K

Obtaining the physical value of spectral radiation intensity, the sensor is responsible for transforming the physical value into digital value for upcoming proceedings. The camera system used in real experiment platform uses Charge-coupled device (CCD) or Complementary Metal-oxide Semiconductor (CMOS) as their sensors. Both sensors transform the photon flux $\phi(\lambda)$ incident on the semiconfuctor into photocurrent I_{ph}[12].

$$I_{ph} = q \int_{\lambda} \phi(\lambda) \cdot \eta_{camera}(\lambda) d\lambda \qquad (4.4)$$

With a certain temperature T:

$$\phi(\lambda) = L(\lambda, T) \qquad (4.5)$$

Eq.4.4 is the mathetical description of the transformation. Where $\phi(\lambda)$ denotes photon flux on the sensor, which is equal to the spectral radiation intensity on the sensor $L(\lambda, T)$ as described in Eq.4.5, and $\eta_{camera}(\lambda)$ denotes the total efficiency of the camera in Eq.4.3. q is the sensitivity parameter of the sensor.

4.3.3 Implementation

Similar to the method used to obtain the digital value of spectral radiation intensity in the real experiment, the virtual experiment platform calculates the intensity digital value in 8 channels using the virtual camera by entering the material properties of the point being measured.

Fig.10 shows the working procedure of the virtual experiment platform. To enable the virtual experimental platform to run on various devices, the entire platform has been implemented using Python as the programming language and packaged into a .py file. Furthermore, all functions have been vectorized to facilitate the generation of image outputs resembling those captured by a physical camera. Additionally, the parallel computing package in Python has been utilized to minimize computation time.
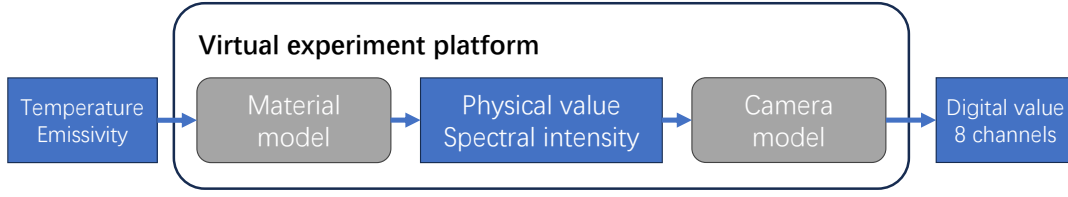
Figure 10: Procedure of using virtual experiment platform to generate digital values

4.4   Temperature estimation algorithm

After obtaining the experimental data calculated by the virtual experiment platform, a temperature estimation algorithm should be developed to calculate the temperature of the measured point based on the experimental data.

Similar to the set up in real experiments, the parameters of the camera model can be considered as known in the virtual experimental platform mentioned in this article. This will on the one hand improve the accuracy of the temperature estimation algorithm and on the other hand avoid some unnecessary complexity.

Thus, in this temperature estimation algorithm, the known variable is the digital value of spectral intensity captured by camera model in virtual experiment platform, the characteristic of the camera system. The variables to be estimated are the temperature of the measured point and its emissivity.
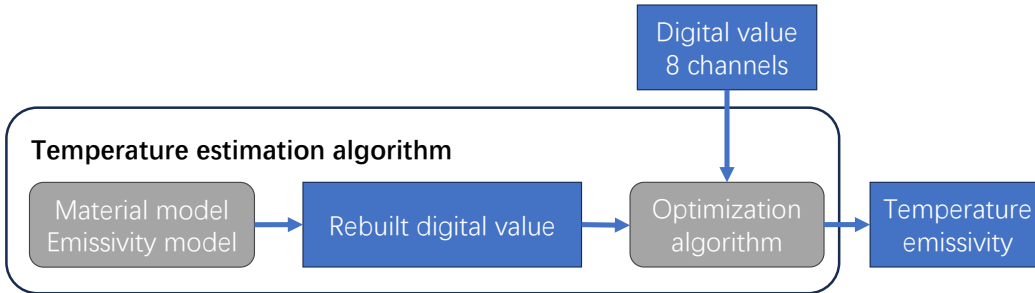

Figure 11: Procedure of temperature estimation algorithm

Fig.11 shows the proceeding procedure of the temperature estimation algorithm. The digital value of the spectral radiation intensity ($I_{rec}(i)$) in the i_{th} channel should be reconstructed in Eq.4.6:

$$I_{rec}(i) = q \int B(\lambda, T) \cdot \varepsilon(\lambda, k, T) \cdot \eta_{camera}(i) d\lambda \tag{4.6}$$

With $I_{DV}(i)$ the reconstructed digital value in i_{th} channel, $B(\lambda, T)$ the black body radiation, $\varepsilon(\lambda, k, T)$ the emissivity model in temperature estimation algorithm, $\eta_{camera}(i)$ the total camera efficiency of i_{th} channel. It can be found that the emissivity model have an additional parameter k, this parameter is used for fitting the emissivity behavior of the measured material. More details can be found in the following section.

Given an initial guess of the status parameters, namely temperature(T_0) and parameters in

emissivity model(k_0). Then, an curve fit algorithm is applied to minimize the difference between the reconstructed digital value (I_{rec}) and the actual digital value (I_{act}) in Eq.4.7.

$$\min_{k,T} \sum_{i=1}^{8} F(I_{rec}(i), I_{act}(i)) \tag{4.7}$$

$F(I_{rec}(i), I_{act}(i))$ is the cost function of the curve fit algorithm. In this application, Non-linear least squares method is used to obtain the optimum parameters as Eq.4.8.

$$F(I_{rec}(i), I_{act}(i)) = (I_{rec}(i) - I_{act}(i))^2 \tag{4.8}$$

After obtaining the estimated temperature ($T_{estimate}$) and the parameter (k) in the emissivity model, the data will be saved in a .xlsx file for potential operations.

4.5   Emissivity model in temperature estimation algorithm

As an unknown quantity in the temperature estimation algorithm, the nature of emissivity as a function of wavelength also introduces an additional degree of freedom into the overall calculation process. In order to provide a more general description of the trend of emissivity with wavelength, an additional parameter (k) in the emissivity model used for temperature estimation has been introduced.

Due to the inherent complexity of this trend, it is often impossible to describe the emissivity using a single parameter. Therefore, the parameter (k) is normally represented as a vector composed of multiple variables. This approach allows for both a concise mathematical representation and the incorporation of more intricate emissivity models into the temperature estimation algorithm.

5 Application and validation

After the theoretical basis of the virtual experiment platform is known and the program of the virtual experiment platform is built, the application should be verified with experiment data generated based on the real experiment.
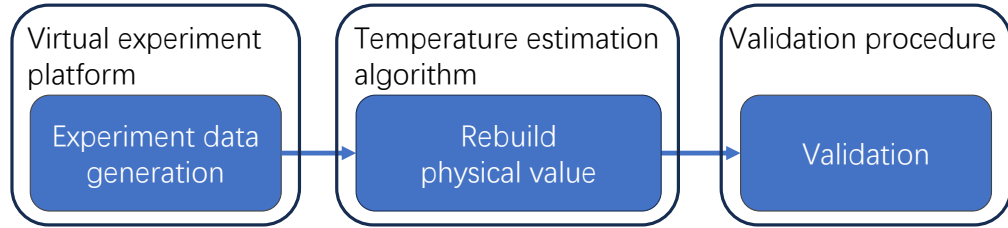

Figure 12: Complete procedure from data generation to model validation

Fig.12 shows the procedure of the application. Firstly, an experiment data set should be generated according to the parameters of the hypothetical material. Then, a temperature estimation algorithm is applied to estimate the temperature of the hypothetical material. Last, a validation procedure is used to check the accuracy and stability of the results of temperature estimation algorithm.

As mentioned in previous sections, these functions is implemented in three programmes. Namely virtual experiment platform, temperature estimation algorithm and validation procedure. Similar to conventional experiment methods, these steps are independent procedures, which means they do not interact with each other.

Accordingly, this chapter will be divided into three sections, which describe the implementation and the parameter settings of the virtual experiment platform, temperature estimation algorithm and validation procedure.
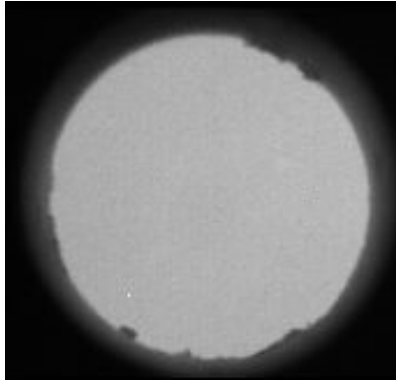
5.1 Experiment data generation

As the first of the three steps mentioned above, it is crucial to generate accurate experimental data correctly. It affects the comparability of the virtual experimental platform with real experiments on the one hand, and the accuracy of the temperature estimation algorithm on the other. As a result, the virtual experimental platform should be able to perform calculations for as many hypothetical materials with different properties as possible.

In order to be able to obtain image similar to image from real camera, the area that the virtual camera is able to capture is set to a 50*50 pixel picture. Fig13 shows the image obtained from real experiment and virtual experiment platform. The major difference between these two images is the coloring. In real experiment, the raw image was saved as a .tiff file, which obtain the spectral intensity received by the specific channel. Then, the intensity is expressed as brightness of the pixel in the display of the image. This results in the experiment data that is not intuitive and requires specialised software to open these data.

As a result, there are a number of optimisations that have been applied in this virtual

experiment platform. Firstly, the raw digital value of the received spectral intensity was saved in an .xlsx file, which simplifies the reading of the data as well as the conversion. In addition, a .jpg image of each channel similar to the real experiment data is also saved. Different from the real experiment data, colours are used here to indicate the value of the spectral intensity. This improves the readability of the experiment data.
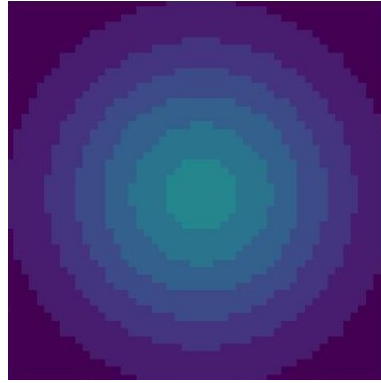
(a) Real experiment data (channel 1)   (b) Virtual experiment data (channel 1)

Figure 13: Comparison between real experiment data at $1300K$ (a) and virtual experiment data at $1098K$ (b)

5.1.1   Temperature field

5.1.2   Emissivity model

5.1.3   Integration method

5.2   Rebuild Physical value

5.2.1   Emissivity model used for calculation

5.2.2   Curve fit algorithm

5.2.3   Parameters in calculation

quantum efficiency, lens factor

5.3   Validation

6 Calcualtion results and analysis

6.1 Calculation results

6.1.1 Temperature field

6.1.2 Emissivity field

6.2 Data analysis

6.2.1 Sensitivity analysis of emissivity models

6.2.2 Performance between different materials

A Appendices

Hello, here is some text without a meaning. This text should show what a printed text will look like at this place. If you read this text, you will get no information. Really? Is there no information? Is there a difference between this text and some nonsense like "Huardest gefburn"? Kjift – not at all! A blind text like this gives you information about the selected font, how the letters are written and an impression of the look. This text should contain all letters of the alphabet and it should be written in of the original language. There is no need for special content, but the length of words should match the language.

This is the second paragraph. Hello, here is some text without a meaning. This text should show what a printed text will look like at this place. If you read this text, you will get no information. Really? Is there no information? Is there a difference between this text and some nonsense like "Huardest gefburn"? Kjift – not at all! A blind text like this gives you information about the selected font, how the letters are written and an impression of the look. This text should contain all letters of the alphabet and it should be written in of the original language. There is no need for special content, but the length of words should match the language.

And after the second paragraph follows the third paragraph. Hello, here is some text without a meaning. This text should show what a printed text will look like at this place. If you read this text, you will get no information. Really? Is there no information? Is there a difference between this text and some nonsense like "Huardest gefburn"? Kjift – not at all! A blind text like this gives you information about the selected font, how the letters are written and an impression of the look. This text should contain all letters of the alphabet and it should be written in of the original language. There is no need for special content, but the length of words should match the language.

After this fourth paragraph, we start a new paragraph sequence. Hello, here is some text without a meaning. This text should show what a printed text will look like at this place. If you read this text, you will get no information. Really? Is there no information? Is there a difference between this text and some nonsense like "Huardest gefburn"? Kjift – not at all! A blind text like this gives you information about the selected font, how the letters are written and an impression of the look. This text should contain all letters of the alphabet and it should be written in of the original language. There is no need for special content, but the length of words should match the language.

Hello, here is some text without a meaning. This text should show what a printed text will look like at this place. If you read this text, you will get no information. Really? Is there no information? Is there a difference between this text and some nonsense like "Huardest gefburn"? Kjift – not at all! A blind text like this gives you information about the selected font, how the letters are written and an impression of the look. This text should contain all letters of the alphabet and it should be written in of the original language. There is no need for special content, but the length of words should match the language.

Glossary

Latex   Generische Mark-up-Sprache zum Erstellen wissenschaftlicher Texte. Sie ist in jeder Hinsicht Word überlegen, welches einem visuellen Mark-Up entspricht. Das X von LaTeX wird als ç (Stimmloser palataler Frikativ) ausgesprochen, vergleiche deutsche Aussprache von *ch*.

TikZ   Frontend-Paket, das auf PGF-Plot aufbaut und zum Erstellen von Graphiken dient.

Tutorial   Kurze Gebrauchsanleitung welche ein Thema, einen gewissen Vorgang oder eine Funktion erklärt. Hat nicht den Anspruch auf Vollständigkeit.

Bibliography

[1] Frazier, W. E., "Metal additive manufacturing: A review", *Journal of Materials Engineering and Performance*, vol. 23, no. 6, pp. 1917–1928, 2014, ISSN: 1544-1024. DOI: 10.1007/s11665-014-0958-z. [Online]. Available: https://link.springer.com/article/10.1007/s11665-014-0958-z.

[2] Swift, K. G. and Booker, J. D., "Rapid prototyping processes", in *Manufacturing process selection handbook*, Swift, K. G. and Booker, J. D., Eds., Amsterdam: Elsevier, 2013, pp. 227–241, ISBN: 9780080993607. DOI: 10.1016/B978-0-08-099360-7.00008-2.

[3] Kruth, J. P., "Material incress manufacturing by rapid prototyping techniques", *CIRP Annals*, vol. 40, no. 2, pp. 603–614, 1991, ISSN: 0007-8506. DOI: 10.1016/S0007-8506(07)61136-6. [Online]. Available: https://www.sciencedirect.com/science/article/pii/s0007850607611366.

[4] Revilla-León, M., Meyer, M. J., and Özcan, M., "Metal additive manufacturing technologies: Literature review of current status and prosthodontic applications", *International Journal of Computerized Dentistry*, pp. 55–67, 2019.

[5] Oliveríra, J., LaLonde, A., and Ma, J., "Processing parameters in laser powder bed fusion metal additive manufacturing", *Materials & Design*, vol. 193, p. 108 762, 2020, ISSN: 0264-1275. DOI: 10.1016/j.matdes.2020.108762. [Online]. Available: https://www.sciencedirect.com/science/article/pii/s0264127520302963.

[6] DebRoy, T., Wei, H. L., Zuback, J. S., Mukherjee, T., Elmer, J. W., Milewski, J. O., Beese, A. M., Wilson-Heid, A., De, A., and Zhang, W., "Additive manufacturing of metallic components – process, structure and properties", *Progress in Materials Science*, vol. 92, no. 5, pp. 112–224, 2018, ISSN: 00796425. DOI: 10.1016/j.pmatsci.2017.10.001.

[7] Li, D., Liu, R., and Zhao, X., *Overview of in-situ temperature measurement for metallic additive manufacturing: How and then what*, 2019. DOI: 10.26153/TSW/17384.

[8] Hagqvist, P., Sikström, F., and Christiansson, A.-K., "Emissivity estimation for high temperature radiation pyrometry on ti–6al–4v", *Measurement*, vol. 46, no. 2, pp. 871–880, 2013, ISSN: 02632241. DOI: 10.1016/j.measurement.2012.10.019.

[9] Pixner, F., Buzolin, R., Schönfelder, S., Theuermann, D., Warchomicka, F., and Enzinger, N., "Contactless temperature measurement in wire-based electron beam additive manufacturing ti-6al-4v", *Welding in the World*, vol. 65, no. 7, pp. 1307–1322, 2021, ISSN: 1878-6669. DOI: 10.1007/s40194-021-01097-0. [Online]. Available: https://link.springer.com/article/10.1007/s40194-021-01097-0.

[10] Bammer, F., Holzinger, B., Humenberger, G., Schuöcker, D., and Schumi, T., "Integration of high power lasers in bending tools", *Physics Procedia*, vol. 5, pp. 205–209, 2010, ISSN: 18753892. DOI: 10.1016/j.phpro.2010.08.045.

[11] Kuhn, T. S., *Black-Body Theory and the Quantum Discontinuity, 1894-1912*. University of Chicago Press, 1987, ISBN: 9780226458007.

[12] Fossum, E. R. and Hondongwa, D. B., "A review of the pinned photodiode for ccd and cmos image sensors", *IEEE Journal of the Electron Devices Society*, vol. 2, no. 3, pp. 33–43, 2014. DOI: 10.1109/JEDS.2014.2306412.

List of Abbreviations

AM	Additive Manufacturing
AP	Arbeitspaket
CCD	Charge-coupled device
CMOS	Complementary Metal-oxide Semiconductor
LBAM	Professorship Laser-based Additive Manufacturing
MSI	Multispectral Imaging
PBF-LB/M	Laser-based Powder Bed Fusion of Metals
ROS	Robot Operating System
SLS	Selective Laser Sintering

Disclaimer

I hereby declare that this thesis is entirely the result of my own work except where otherwise indicated. I have only used the resources given in the list of references.

Garching, July 31, 2023

_____
(Signature)